

Rational Design of Single-Chain Polymeric Nanoparticles that Kill Planktonic and Biofilm Bacteria

Thuy-Khanh Nguyen, Shu Jie Lam, Kitty Ka Kit Ho, Naresh Kumar, Greg G. Qiao, Suhelen Egan, Cyrille Boyer, and Edgar H. H. Wong

ACS Infect. Dis., **Just Accepted Manuscript** • DOI: 10.1021/acsinfecdis.6b00203 • Publication Date (Web): 30 Jan 2017

Downloaded from <http://pubs.acs.org> on February 1, 2017

Just Accepted

“Just Accepted” manuscripts have been peer-reviewed and accepted for publication. They are posted online prior to technical editing, formatting for publication and author proofing. The American Chemical Society provides “Just Accepted” as a free service to the research community to expedite the dissemination of scientific material as soon as possible after acceptance. “Just Accepted” manuscripts appear in full in PDF format accompanied by an HTML abstract. “Just Accepted” manuscripts have been fully peer reviewed, but should not be considered the official version of record. They are accessible to all readers and citable by the Digital Object Identifier (DOI®). “Just Accepted” is an optional service offered to authors. Therefore, the “Just Accepted” Web site may not include all articles that will be published in the journal. After a manuscript is technically edited and formatted, it will be removed from the “Just Accepted” Web site and published as an ASAP article. Note that technical editing may introduce minor changes to the manuscript text and/or graphics which could affect content, and all legal disclaimers and ethical guidelines that apply to the journal pertain. ACS cannot be held responsible for errors or consequences arising from the use of information contained in these “Just Accepted” manuscripts.

Rational Design of Single-Chain Polymeric Nanoparticles that Kill Planktonic and Biofilm Bacteria

Thuy-Khanh Nguyen,¹ Shu Jie Lam,² Kitty K. K. Ho,³ Naresh Kumar,³ Greg G. Qiao,² Suhelen Egan,⁴ Cyrille Boyer,^{1,*} and Edgar H. H. Wong^{1,*}

¹Centre for Advanced Macromolecular Design (CAMD) and Australian Centre for NanoMedicine (ACN), School of Chemical Engineering, UNSW Australia, Sydney NSW 2052, Australia. ²Department of Chemical and Biomolecular Engineering, The University of Melbourne, Parkville VIC 3010, Australia. ³School of Chemistry, UNSW Australia, Sydney NSW 2052, Australia. ⁴Centre for Marine Bio-Innovation, School of Biological, Earth and Environmental Sciences, UNSW Australia, Sydney NSW 2052, Australia.

KEYWORDS: single-chain polymeric nanoparticles, self-folding, RAFT polymerization, antibiotics, biofilm

ABSTRACT: Infections caused by multidrug-resistant bacteria are on the rise and as such, new antimicrobial agents are required to prevent the onset of a post-antibiotic era. In this study, we develop new antimicrobial compounds in the form of single-chain polymeric nanoparticles (SCPNs) that exhibit excellent antimicrobial activity against Gram-negative bacteria (e.g., *Pseudomonas aeruginosa*) at μM concentrations (e.g., 1.1 μM), and remarkably kill $\geq 99.99\%$ of both planktonic cells and biofilm within an hour. Linear random copolymers, which comprise of oligoethylene glycol (OEG), hydrophobic and amine groups, undergo self-folding in aqueous due to intramolecular hydrophobic interactions to yield these SCPNs. By systematically varying the hydrophobicity of the polymer, we can tune the extent of cell membrane wall disruption which in turn governs the antimicrobial activity and rate of resistance acquisition in bacteria. We also show that the incorporation of OEG groups into the polymer design is essential in preventing complexation with proteins in biological medium, thereby maintaining the antimicrobial efficacy of the compound even in *in vivo* mimicking conditions. In comparison to the last resort antibiotic colistin, our lead agents have higher therapeutic index (by ca. 2-3 times) and hence better biocompatibility. We believe that the SCPNs developed here have potential for clinical applications and the information pertaining to their structure-activity relationship will be valuable towards the general design of synthetic antimicrobial (macro)molecules in the future.

INTRODUCTION

The prolonged misuse of antibiotics in therapeutics and animal husbandry has led to the rise of multidrug resistance in bacteria, which is now considered a critical global healthcare issue. By 2050, it is anticipated that drug-resistant infections could cause 10 million deaths worldwide, while costing the global economy up to \$100 trillion.¹ The severity of this issue is further compounded by the dearth of new antimicrobial agents to combat multidrug-resistant bacteria.²⁻⁴ Given that antibiotic resistance is developing faster than the introduction of new antimicrobial agents, there exists an urgent need for developing new and effective compounds.⁵

Most antibiotics were discovered from the 1940s to 1960s during the screening of cultivable microorganisms in the laboratory, and they occur as chemical compounds secreted by a particular microorganism that exhibited toxicity (i.e., antimicrobial properties) toward other microbial species.⁶ Since the screening of available cultivable microorganisms was exhausted in the 1960s, the discovery of new antibiotics remained few and far between. As a

rare example, in 2015, a new antibiotic named teixobactin⁷ was discovered using iChip (isolation chip),⁸ which allows the screening of soil microorganisms that were previously uncultivable in the laboratory. While the use of natural product discovery methods has been the benchmark for antimicrobial discovery, the application of synthetic approaches warrants consideration as potential alternatives for the development of new antimicrobial agents because of: i) the laborious and time-consuming process associated with biological screenings; and ii) the advancements in modern synthetic chemistry, controlled polymerization⁹⁻¹² in particular.

Inspired by (naturally-occurring) antimicrobial peptides (AMPs), various antimicrobial polymers have been developed using controlled polymerization strategies, mostly to mimic the innate amphiphilic structure of AMPs,¹³⁻²¹ which is responsible for their bactericidal properties through physical cell membrane disruption. This mode of mechanism minimizes the likelihood of resistance development in bacteria, making AMPs particularly attractive for combating antibiotic-resistant bacteria.²² Although AMPs and synthetic mimics thereof

demonstrate good antimicrobial activity against planktonic microbial cells, the majority of these materials unfortunately suffer from low biocompatibility with mammalian cells, poor in vivo efficacy, and lack of activity against biofilms, thereby precluding them from potential clinical applications. Only a handful of synthetic antimicrobial macromolecules have truly overcome some of these challenges. For instance, several reports have recently demonstrated the formulation of polymer nanoparticles (i.e., star-shaped polymers²³⁻²⁵ or micelles²⁶) can increase antimicrobial activity and improve mammalian cell biocompatibility.

The limitations concerning current antimicrobial polymeric systems are not due to the methodologies used in synthesizing the materials. This is especially true considering the technological revolution in synthetic polymer chemistry over the last few decades has enabled the synthesis of biomaterials with precise properties (e.g., composition, functionality and topology).²⁷⁻²⁸ The biggest challenge however lies with designing a polymer with the appropriate balance of amphiphilicity and selectivity such that it will preferentially disrupt membranes of bacteria cells and not those of mammalian cells. In addition, as antimicrobial polymers and AMPs are usually cationic, complexation with proteins found in biological fluids are almost unavoidable, and this can negatively impact the in vivo efficacy of the materials – a point that has been largely overlooked.²⁹ Thus, further investigations into the rational design of antimicrobial polymers are necessary to address these challenges.

Here, we report the development of novel antimicrobial single-chain polymeric nanoparticles (SCPNS) as potential drug candidates (Figure 1a). The formation of SCPNs via controllable self-folding of linear polymer chains has been

attracting great scientific interests recently because of the possibility in emulating the reversible self-folding process of natural biomolecules that have controlled monomer sequences (e.g., proteins and peptides), which is integral to their biological functions.³⁰⁻³² Although current SCPNs have yet to rival the structural complexity and function of natural biomolecules, they are nevertheless discrete and possess nanocompartments within their structure which may enable them to act as catalytic nanoreactors or drug carriers. Various strategies are available to form SCPNs, including the use of (dynamic) covalent³³⁻⁴⁰ and non-covalent bonds.⁴¹⁻⁴⁵ Our SCPNs are stabilized by intramolecular hydrophobic interactions in aqueous, where the hydrophobic motifs have a dual purpose of contributing to the formation of SCPNs and endowing the nanoparticles with antimicrobial properties. By systematically varying the chemical compositions, we identify SCPNs that preferentially target bacteria over mammalian cells, and without invoking substantial resistance development in bacteria. Furthermore, the incorporation of oligoethylene glycol (OEG) side chains enable the SCPNs to maintain antimicrobial activity even in the presence of serum, highlighting the importance of incorporating low-fouling components to minimize unwanted protein complexation. Crucially, the SCPNs can kill both planktonic microbial cells and biofilm, unlike most AMPs and traditional antibiotics which are ineffective against biofilm. Interestingly, the SCPNs also cause the dispersal of biofilm, which is highly advantageous for treating biofilm-related infections. Thus, this study not only suggests the potential utility of antimicrobial SCPNs for clinical applications but also provides valuable information on the structure-activity relationship for the optimization of future antimicrobial polymer systems.

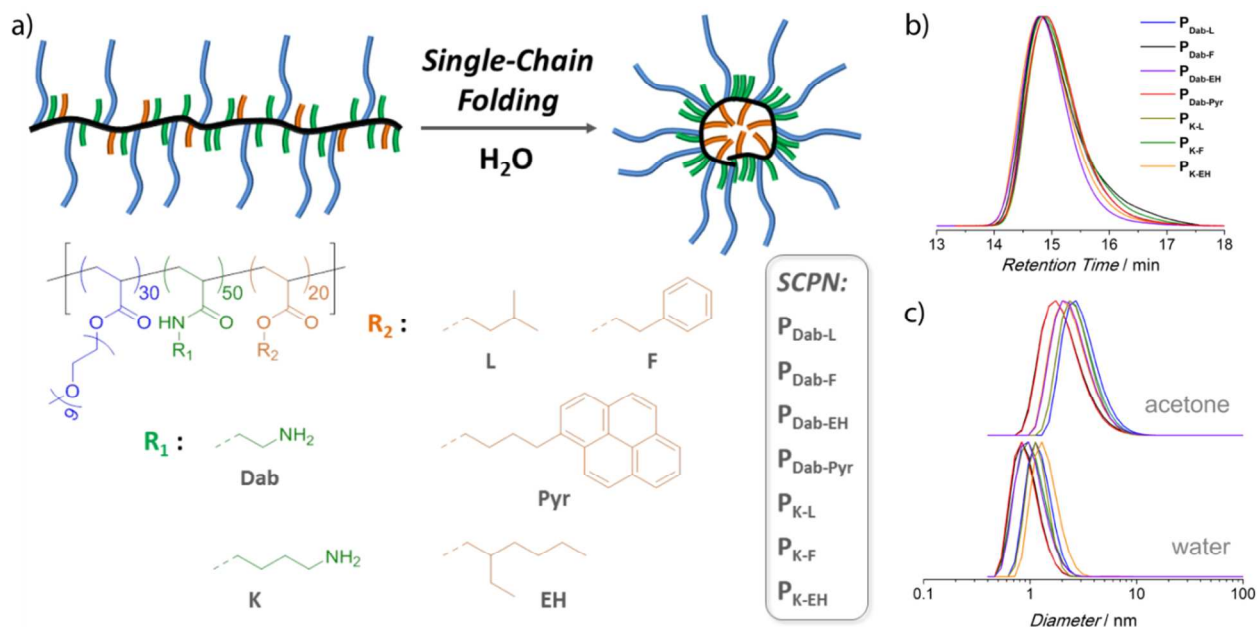


Figure 1. (a) Single-chain folding of amphiphilic random copolymers to form antimicrobial SCPNs in water. The compositional structures of the SCPNs include oligoethylene glycol side chains plus various combinations of amino and hydrophobic groups. (b) GPC differential refractive index chromatograms of the Boc-protected polymers as prepared via RAFT polymerization. (c) DLS volume distributions of the deprotected polymers in acetone and water.

EXPERIMENTAL SECTION

Materials. Ethylenediamine (Sigma-Aldrich, $\geq 99\%$), 1,4-diaminobutane (Aldrich, 99%), di-*tert*-butyl dicarbonate (Aldrich, 99%), triethylamine (Scharlau, 99%), acryloyl chloride (Merck, $\geq 96\%$), isoamyl alcohol (Aldrich, $\geq 98\%$), 2-phenylethanol (Aldrich, $\geq 99\%$), 1-pyrenebutanol (Aldrich, 99%), oligoethylene glycol methyl ether acrylate (OEGA) M_n 480 g mol⁻¹ (Aldrich), trifluoroacetic acid (TFA) (Sigma-Aldrich, 99%), chloroform (VWR Chemicals), hexane (Merck), diethyl ether (Merck) and basic alumina (Al₂O₃) (LabChem) were used as received. 2,2'-azobis(2-methylpropionitrile) (AIBN) (Acros, 98%) was purified by recrystallization from methanol. Sodium sulfate (Na₂SO₄), magnesium sulfate (MgSO₄), sodium hydrogen carbonate (NaHCO₃), tetrahydrofuran, 1,4-dioxane, methanol and acetone were obtained from Chem-Supply and used as received. Milli-Q water with a resistivity of > 18 M Ω -cm was obtained from an in-line Millipore RiOs/Origin water purification system.

Characterizations of Synthetic (Macro)molecules. ¹H and ¹³C nuclear magnetic resonance (NMR) spectroscopy were conducted on a Bruker AC300F spectrometer using deuterated solvents (obtained from Cambridge Isotope Laboratories) as reference solvents and at a sample concentration of ca. 10-20 mg mL⁻¹.

Gel permeation chromatography (GPC) was carried out on a Shimadzu liquid chromatography system equipped with a Shimadzu refractive index detector and two MIX C columns (Polymer Lab) operating at 40 °C. Tetrahydrofuran was used as the eluent at a flow rate of 1 mL min⁻¹. The system was calibrated with polystyrene standards with molecular weights of 200 to 10⁶ g mol⁻¹.

Dynamic light scattering (DLS) and zeta-potential measurements were performed using a Malvern Zetasizer Nano ZS apparatus equipped with a He-Ne laser operated at $\lambda = 633$ nm and at a scattering angle of 173°. All samples were measured at a polymer concentration of ca. 4-5 mg mL⁻¹ where the solvents used to solubilize the polymers were filtered through a 0.45 μ m pore size filter prior to sample preparation.

For atomic force microscopy (AFM) analysis, 5 μ L of polymer solution (5 μ g mL⁻¹ in Milli-Q water) was drop-casted onto a freshly cleaned silicon wafer and allowed to dry in vacuo overnight prior to analysis. AFM analysis was performed on a Bruker Dimension ICON SPM instrument. A silicone cantilever was used in Contact Mode at 600 \times 600 nm scan size and 0.5 Hz scan rate.

Synthesis of Cationic Monomers. The synthesis of cationic monomers *tert*-butyl (2-acrylamidoethyl) carbamate and *tert*-butyl (4-acrylamidobutyl) carbamate, which mimic the amino acids diaminobutyric acid (Dab) and lysine (K) respectively, proceeded in two steps. Firstly, ethylenediamine or 1,4-diaminobutane (0.3 mol) was dissolved in chloroform (300 mL), followed by the dropwise addition of di-*tert*-butyl dicarbonate (0.03 mol in 150 mL) over 2 h at 0-5 °C. The reaction mixture was stirred for another 20 h at 25 °C. White precipitates were filtered, and the organic phase was washed exhaustively with wa-

ter (6 \times 250 mL) to remove excess diamines. The organic layer was then dehydrated over Na₂SO₄, filtered and dried in vacuo. The intermediate product was used immediately in the next step without further purification.

Tetrahydrofuran (150 mL) was added to dissolve the intermediate product. Triethylamine (36 mmol) and acryloyl chloride (31.5 mmol) were added dropwise to the solution at 0-5 °C with N₂ bubbling. The contents were stirred at 25 °C for 1 h. The urea by-products were filtered and the solvent was removed in vacuo. The crude product was dissolved in chloroform (150 mL) and washed against brine (1 \times 75 mL). The organic phase was stirred with MgSO₄ and basic Al₂O₃ for 10 min, filtered, and concentrated in vacuo. The product was further purified by repeated precipitation steps (twice) in hexane to yield the *tert*-butyloxycarbonyl Boc-protected monomer as fine white powder, which was dried in vacuo. The yields for *tert*-butyl (2-acrylamidoethyl) carbamate and *tert*-butyl (4-acrylamidobutyl) carbamate were ca. 2.0 g (31 mol%) and 2.4 g (33 mol%), respectively.

tert-butyl (2-acrylamidoethyl) carbamate; ¹H NMR (300 MHz, CDCl₃, 25 °C): δ_H (ppm) = 6.56 (br s, 1H, NH), 6.28 (dd, $J = 17.1$ Hz, 1.5 Hz, 1H, CHH=CH), 6.12 (dd, $J = 17.1$ Hz, 10.2 Hz, 1H, CHH=CH), 5.65 (dd, $J = 10.2$ Hz, 1.5 Hz, 1H, CHH=CH), 5.05 (br s, 1H, NH), 3.49-3.41 (m, 2H, CH₂), 3.34-3.28 (m, 2H, CH₂), 1.45 (s, 9H, CH₃). ¹³C NMR (300 MHz, CDCl₃, 25 °C): δ_C (ppm) = 166.23, 157.50, 130.88, 126.30, 79.85, 41.05, 40.09, 28.35.

tert-butyl (4-acrylamidobutyl) carbamate; ¹H NMR (300 MHz, CDCl₃, 25 °C): δ_H (ppm) = 6.28 (dd, $J = 17.1$ Hz, 1.5 Hz, 1H, CHH=CH), 6.20 (br s, 1H, NH), 6.12 (dd, $J = 17.1$ Hz, 10.2 Hz, 1H, CHH=CH), 5.63 (dd, $J = 10.2$ Hz, 1.5 Hz, 1H, CHH=CH), 4.70 (br s, 1H, NH), 3.40-3.30 (m, 2H, CH₂), 3.19-3.10 (m, 2H, CH₂), 1.44 (s, 9H, CH₃). ¹³C NMR (300 MHz, CDCl₃, 25 °C): δ_C (ppm) = 165.70, 156.22, 130.97, 126.17, 79.29, 40.08, 39.21, 28.42, 27.74, 26.50.

Synthesis of Hydrophobic Monomers. A standard procedure was employed for the synthesis of hydrophobic monomers isoamyl acrylate, 2-phenylethyl acrylate and 4-(pyren-1-yl) butyl acrylate. As an example, 2-phenylethanol (17.7 mmol) was dissolved in tetrahydrofuran (100 mL). Triethylamine (23.0 mmol) and acryloyl chloride (21.2 mmol) were then added to this solution in a dropwise manner at 0-5 °C with N₂ bubbling. The mixture was stirred at 25 °C for 5 h. The urea by-products were filtered and the solvent was removed in vacuo. The crude product was dissolved in chloroform (150 mL) and washed sequentially with 0.1 M HCl solution (1 \times 75 mL), saturated NaHCO₃ (1 \times 75 mL), brine (1 \times 75 mL) and water (1 \times 75 mL). The organic phase was stirred with MgSO₄ and basic Al₂O₃ for 10 min, filtered, and dried in vacuo to yield the monomer as a colorless liquid. The yields for the monomers were between 70 to 80 mol%.

Isoamyl acrylate; ¹H NMR (300 MHz, CDCl₃, 25 °C): δ_H (ppm) = 6.39 (dd, $J = 17.4$ Hz, 1.5 Hz, 1H, CHH=CH), 6.11 (dd, $J = 17.4$ Hz, 10.5 Hz, 1H, CHH=CH), 5.80 (dd, $J = 10.2$ Hz, 1.8 Hz, 1H, CHH=CH), 4.18 (dd, $J = 6.9$ Hz, 2H, CH₂O), 1.60-1.52 (m, 2H, CH₂CH₂O), 0.93 (d, 6H, CH₃). ¹³C NMR

(300 MHz, CDCl₃, 25 °C): δ_c (ppm) = 169.88, 130.67, 128.50, 67.90, 31.59, 22.65, 20.59, 14.12.

2-Phenylethyl acrylate; ¹H NMR (300 MHz, CDCl₃, 25 °C): δ_H (ppm) = 7.35-7.23 (m, 5H, aromatic), 6.42 (dd, *J* = 17.1 Hz, 1.5 Hz, 1H, CHH=CH), 6.14 (dd, *J* = 17.4 Hz, 10.5 Hz, 1H, CHH=CH), 5.84 (dd, *J* = 10.5 Hz, 1.5 Hz, 1H, CHH=CH), 4.41 (dd, *J* = 7.2 Hz, 2H, CH₂O), 3.02 (dd, *J* = 7.2 Hz, 2H, CH₂C₆H₅). ¹³C NMR (300 MHz, CDCl₃, 25 °C): δ_c (ppm) = 166.13, 137.80, 134.64, 130.74, 128.94, 128.53, 128.48, 127.51, 126.60, 65.04, 35.13.

4-(Pyren-1-yl) butyl acrylate acrylate; ¹H NMR (300 MHz, CDCl₃, 25 °C): δ_H (ppm) = 8.28-7.80 (m, 9H aromatic), 6.44 (dd, *J* = 17.1 Hz, 1.5 Hz, 1H, CHH=CH), 6.15 (dd, *J* = 17.4 Hz, 10.2 Hz, 1H, CHH=CH), 5.84 (dd, *J* = 10.2 Hz, 1.5 Hz, 1H, CHH=CH), 4.28 (dd, *J* = 6.3 Hz, 2H, CH₂O), 3.42 (dd, *J* = 7.8 Hz, 2H, CH₂C₆H₅), 2.08-1.86 (m, 4H, CH₂CH₂). ¹³C NMR (300 MHz, CDCl₃, 25 °C): δ_c (ppm) = 166.35, 136.32, 131.46, 130.92, 130.65, 129.90, 128.64, 128.56, 127.52, 127.32, 127.25, 126.67, 125.85, 125.13, 125.05, 124.93, 124.83, 124.75, 123.30, 64.41, 33.05, 30.36, 28.65.

General RAFT Polymerization and Procedure for Removal of Protecting Groups. Typically, the synthesis of all linear polymer precursors followed the same protocol. The RAFT agent benzyl dodecyl carbonotrithioate³⁶ (9.0 μmol), AIBN (4.5 μmol), OEGA (272 μmol), cationic monomer (453 μmol), and hydrophobic monomer (181 μmol) were dissolved in 1,4-dioxane (such that the total monomer concentration in solvent is 1 M). The solution was degassed by bubbling with N₂ for 20 min. The reaction mixture was then stirred at 70 °C for 20 h under N₂ atmosphere before cooling in an ice bath. Aliquots were taken for ¹H NMR analysis. The mixture was diluted with acetone (ca. 2 mL) and precipitated into hexane:diethyl ether (7:3, 12 mL). The precipitate was isolated by centrifugation, dissolved in acetone, and precipitated once more. The Boc-protected polymers were dried in vacuo prior to analysis.

The Boc protecting groups were subsequently removed using TFA. In general, the polymer was dissolved in dichloromethane (ca. 7 wt% polymer), followed by the addition of TFA (20 mol equivalent with respect to the Boc group). The mixture was stirred at 25 °C for 3 h and subsequently precipitated into diethyl ether:hexane (4:1). The precipitate was isolated by centrifugation, dissolved in methanol, and reprecipitated twice more. The polymer was then dried in vacuo and further purified by dialysis in water using a Vivaspin[®] Turbo 15 (Sartorius) centrifugal concentrator with a molecular weight cutoff of 3 kDa. The aqueous solution was lyophilized to yield the Boc-protected polymer. The yields for the final polymers were between 65 to 80 mol%.

Mammalian Cell Viability Studies. Rat H4IIE cells were cultivated in DMEM medium (supplemented with 10% FBS, 1 × GlutaMAX[™], and 1 × penicillin-streptomycin) in a humidified atmosphere containing 5% CO₂ at 37 °C. Cells were seeded in a T75 flask (ca. 3 × 10⁶ cells mL⁻¹) and passaged twice a week prior to the performance of the subsequent cell viability studies.

H4IIE cells were grown to 80% confluence and trypsinised prior to assay. The cells were counted on a cell counter (Coulter Particle Counter Z series, Beckman Coulter), diluted with “complete” DMEM medium and seeded in a 96-well plate at a density of 10000 cells per well. The cells were incubated at 37 °C in 5% CO₂ for 24 h. Spent medium was removed. Varying concentrations of SCPNs and colistin were prepared in ‘complete’ DMEM medium (100 μL) and incubated with cells at 37 °C in 5% CO₂ for a further 24 h. Next, 20 μL of MTS solution was added to each well. Plates were further incubated at 37 °C in 5% CO₂ for 2 h. The absorbance at 490 nm was measured with a plate reader (PerkinElmer 1420 Multilabel Counter VICTOR[®]). Two independent runs of the assay were conducted and two replicates were used in each run for each material concentration. Cells that were untreated were used as positive growth control.

Percentage viability of cells was calculated using the following formula:

$$\% \text{ viability} = \left(\frac{A_{490} \text{ test sample} - A_{490} \text{ background}}{A_{490} \text{ cells alone} - A_{490} \text{ background}} \right) \times 100$$

where A_{490} refers to the absorbance value at a wavelength of 490 nm.

Hemolysis Studies. Hemolytic activity of the polymers was assessed using fresh sheep red blood cells (RBCs). RBCs were diluted 1:20 in PBS (pH 7.4), pelleted by centrifugation and washed three times in PBS (1000g, 10 min). The RBCs were then resuspended to achieve 5% (v/v) in PBS. Different concentrations of polymers (150 μL) were prepared in sterilized tubes, followed by the addition of the RBCs suspension (150 μL). The highest polymer concentration tested was 2 mg mL⁻¹. PBS buffer was used as a negative control while Triton-X 100 (1% v/v in PBS) was used as positive hemolysis control. The tubes were incubated for 2 h at 37 °C and 150 rpm shaking speed in an incubator. Following incubation, the tubes were centrifuged (1000g, 8 min) and aliquots of the supernatants (100 μL) were transferred into a 96-well microplate where the absorbance values were monitored at 485 nm using a microtiter plate reader (FLUOstar Omega, BMG Labtech). The percentage of hemolysis was calculated using the absorbance values and the formula below:

$$\% \text{ Hemolysis} = (A_{\text{polymer}} - A_{\text{negative}}) / (A_{\text{positive}} - A_{\text{negative}}) \times 100\%$$

Minimum Inhibitory Concentration (MIC) Determination. MIC was determined by broth microdilution method according to Clinical and Laboratory Standards Institute (CLSI) guidelines. Briefly, bacterial culture was grown from a single colony in 10 mL of Mueller-Hinton broth (MHB) at 37 °C with shaking at 200 rpm overnight. The subculture was prepared from the overnight culture by diluting 1:100 in 5 mL MHB and allowed to grow to mid-log phase, then diluted to the appropriate concentration for the MIC test. A twofold dilution series of 50 μL of polymers and antibiotics solution in MHB were added into 96-well microplates followed by the addition of 50 μL of the subculture suspension. The final concentration of bacteria in each well was ca. 5 × 10⁵ cells mL⁻¹. The plates were incubated at 37 °C for 20 h, and the absorbance at 600 nm was measured with a microtiter plate reader

(Wallac Victor², Perkin-Elmer). MIC values were defined as the lowest concentration of sample that showed no visible growth and inhibited cell growth by more than 90%. Positive controls without polymer and negative controls without bacteria were included. All assays included two replicates and were repeated in at least three independent experiments.

Membrane Potential Measurements. The assays were conducted in M9 minimal medium containing 48 mM Na₂HPO₄, 22 mM KH₂PO₄, 9 mM NaCl, 19 mM NH₄Cl, pH 7.0, supplemented with 2 mM MgSO₄, 100 μM CaCl₂ and 20 mM glucose. The fluorophore DiOC₂(3) was used to determine the red-to-green fluorescence ratio that is indicative of the membrane potential of the bacteria cells. Subculture of PAO₁ was prepared from overnight culture in fresh MHB and allowed to grow to mid-log phase. Cells were then collected by centrifugation, resuspended and adjusted to ca. 2×10^6 CFU mL⁻¹ in M9 medium. A twofold dilution series of 50 μL of polymers and antibiotics solution in M9 medium were added into 96-well microplates (black with clear bottom) followed by the addition of 50 μL of DiOC₂(3) solution (30 μM in Milli-Q water), and 100 μL of the viable cells solution. The final concentration of bacteria in each well was ca. 5×10^5 cells mL⁻¹. The plates were incubated at 25 °C for 24 h. Membrane potential was determined using a microtiter plate reader (FLUOstar Omega, BMG Labtech) with 485-nm excitation and detection through 520-nm and 620-nm band-pass (ca. 10 nm bandwidth) filters. All assays included two replicates and were repeated in at least two independent experiments.

Antimicrobial Resistance Studies. Resistance studies of *P. aeruginosa* PAO₁ against SCPNs were performed by sequential passaging.⁷ Bacterial cells at exponential phase were diluted to a final concentration with a 600 nm optical density (OD₆₀₀) of 0.01 in 1 mL MHB in the presence of selected SCPNs or antibiotics (i.e., gentamicin and colistin) at subinhibitory concentrations (i.e., $\frac{1}{4} \times$ MIC, $\frac{1}{2} \times$ MIC, $1 \times$ MIC and $2 \times$ MIC). Cells were incubated at 37 °C with shaking at 200 rpm, and passaged at 24 h intervals. After incubation, the cultures were checked for growth. Cultures from the second highest concentrations that allow growth (OD₆₀₀ ≥ 2.00) were diluted to an OD₆₀₀ of 0.01 per mL in fresh MHB containing $\frac{1}{4} \times$ MIC, $\frac{1}{2} \times$ MIC, $1 \times$ MIC and $2 \times$ MIC of polymers or antibiotics. This serial passaging was repeated daily for 22 days. Assays were performed with two independent experiments.

Bacteria Time-Kill Studies. The laboratory strain *P. aeruginosa* PAO₁ was used to investigate the bactericidal property of the SCPNs. Biofilms were grown as described in our previous studies.⁴⁶⁻⁴⁸ Briefly, in all assays, a single colony of PAO₁ was inoculated in 10 mL of Luria Bertani medium (LB 10) at 37 °C with shaking at 200 rpm overnight. The overnight culture was diluted 1:200 in freshly prepared M9 minimal medium containing 48 mM Na₂HPO₄, 22 mM KH₂PO₄, 9 mM NaCl, 19 mM NH₄Cl, pH 7.0, supplemented with 2 mM MgSO₄, 100 μM CaCl₂ and 20 mM glucose. The bacterial suspension was then aliquoted 1 mL per well of tissue-culture treated 24-well plates (Costar, Corning®). The plates were incubated at 37

°C with shaking at 180 rpm in an orbital shaker that does not stop agitation when the door is opened (model OM11, Ratek, Boronia, Australia) and the biofilm cultures were allowed to grow for 6 h without any disruption. SCPNs and colistin were then added to the wells such that the final concentration of $4 \times$ MIC was achieved. For this, 10 μL aliquot from a stock solution of the compound dissolved in sterile Milli-Q water was added to the wells. The plates were incubated for different periods of time, from 1 to 60 min, before quantifying the viability of both planktonic and biofilm bacteria. After treatment, the planktonic and biofilm viability analysis were determined by a drop plate method. For planktonic analysis, free-floating cells in the biofilm supernatant were serially diluted in sterile PBS and plated onto LB agar. For biofilm analysis, cells attached on the interior surfaces of the well (surface area 4.5 cm²) were washed twice with sterile PBS to remove loosely attached bacteria, before being resuspended and homogenized in PBS by incubating in an ultrasonication bath (150 W, 40 kHz; Unisonics, Australia) for 20 min. Re-suspended biofilm cells were then serially diluted and plated onto LB agar. Planktonic and biofilm colonies were counted and CFU was calculated after 24 h incubation at 37 °C. All assays included two replicates and were repeated in at least three independent experiments.

Biofilm Imaging. A single colony of PAO₁ was cultured overnight in 10 mL of LB 10 medium at 37 °C. The resulting bacteria was collected by centrifugation and resuspended in the same volume of LB twice. The OD of the resulting culture was adjusted to OD₆₀₀ = 0.1 in M9 medium. Sterile glass coverslips (No.1, diameter 13 mm, ProSciTech, Australia) were placed individually in 12-well plates followed by the addition of 2 mL of the bacterial suspension. The plates were incubated at 37 °C with shaking at 120 rpm for 18 h. The surfaces were then gently rinsed twice with PBS before being treated with 1 mL of P_{Dab-F} solution in PBS for 1 h at 37 °C with shaking at 120 rpm. Surfaces treated with PBS instead of polymer were used as controls. After incubation, the surfaces were gently rinsed once with PBS followed by staining with LIVE/DEAD BacLight bacterial viability kit reagents (Molecular Probes) according to the manufacturer's procedure. Briefly, 2 μL of each of the two components were mixed thoroughly in 1 mL of PBS, and then 10 μL of the mixture solution was trapped between the sample and the glass microscopy slide. After 10 min of incubation at room temperature in the dark, the samples were observed and imaged with an Olympus FV1200 Confocal Inverted Microscope. Cells that were stained green were considered viable and those that stained red were considered non-viable as well as those that stained both green and red. The assay was repeated in two independent experiments.

Biofilm Dispersal Studies. To characterize the effect of SCPNs on biofilm dispersal, preformed PAO₁ biofilms were grown for 6 h and treated the same manner as in the time-kill study. Biofilm biomass was quantified by using the crystal violet (CV) staining method as previously described.⁴⁶⁻⁴⁸ Briefly, after treatment, the culture supernatant was removed and the biofilm on the well surfaces

was washed once with 1 mL of PBS, followed by the addition of 1 mL 0.03% CV stain made from a 1:10 dilution of Gram crystal violet (BD) in PBS. The plates were incubated on the bench for 20 min before the wells were washed twice with PBS. Photographs of the stained biofilms were obtained with a digital camera. The CV stained biofilms were mixed with 1 mL 100% ethanol and quantified by measuring the OD₅₅₀ of the homogenized suspension using a microtiter plate reader (Wallac Victor², Perkin-Elmer). All assays included two replicates and were repeated in at least three independent experiments.

RESULTS AND DISCUSSION

In this study, a library of amphiphilic SCPNs was generated which consists of three key components, namely OEG, hydrophobic and amino groups (Figure 1a), where some of these functionalities were judiciously chosen to mimic the structure of amino acids (i.e., leucine (L), phenylalanine (F), diaminobutyric acid (Dab) and lysine (K)). Specifically, linear random copolymer precursors were prepared via the reversible addition-fragmentation chain transfer (RAFT) polymerization of acrylate and acrylamide monomers. Based on our experience in synthesizing SCPNs, the targeted number-average degree of polymerization (DP_n) was set at 100, and each polymer chain contained 20 repeat units of hydrophobic groups to induce SCPN formation,³⁶⁻³⁷ while the molar ratio of amino to hydrophobic groups was 2.5:1 to ensure the solubility of SCPNs in aqueous.²³ Further, each polymer chain consisted of 30 repeat units of OEG side chains to minimize interparticle interactions³⁷ besides endowing the polymer with low-fouling properties. It is worthwhile noting that the primary amine of amino-based monomers was protected with *tert*-butyloxycarbonyl (Boc) protecting group prior to RAFT polymerization. This step was necessary for the polymerization to proceed successfully as primary amines can cause aminolysis of RAFT agents.⁴⁹ The Boc groups on the linear polymers were subsequently removed with trifluoroacetic acid (TFA), yielding P_{Dab-L}, P_{Dab-F}, P_{Dab-EH}, P_{Dab-Pyr}, P_{K-L}, P_{K-F} and P_{K-EH}. For simplicity, we named the polymers without the OEG nomenclature and based only on the types of amino and hydrophobic groups present in the polymer (note that amino acid abbreviations were used for functional groups that bear structural resemblance to amino acid).

In general, the RAFT polymerizations were well-controlled in all cases, as GPC analysis of the Boc-protected linear polymer precursors produced monomodal molecular weight distributions with dispersity (*D*) values of ca. 1.2-1.3 (Figure 1b, Table 1). It is important to note that the number-average molecular weight (*M*_n) values of the polymers obtained from GPC measurements were relative to polystyrene calibration standards and as such only serve as estimates. For a more accurate determination of the molecular weights of the polymers, NMR analysis based on the monomer conversion was applied. ¹H NMR analysis revealed that the polymerizations proceeded with quantitative (> 95%) monomer conversion after 20 h, as evidenced by the disappearance of resonances

corresponding to the vinyl protons at δ_H 5.7-6.4 ppm. This suggested that the obtained DP_n was close to the targeted value of 100. Further analysis of the NMR spectra based on the RAFT terminal groups also confirmed the DP_n of the polymers as ca. 100. In addition, the chemical compositions of the polymers were confirmed to be similar to the molar feed ratio. Treatment with TFA resulted in the removal of Boc groups as verified by the disappearance of methyl protons at δ_H 1.45 ppm (Figure S1-S7, Supporting Information (SI)).

The formation of SCPNs in water relies on the ability of the hydrophobic motifs to drive the collapse of single polymer chains into unimer micelles. To establish this, DLS measurements were performed to measure the average hydrodynamic diameter (*D*_h) of the polymers under two different solvent conditions: one in water where SCPNs will form, and the other in acetone for which all the functional groups are soluble in and the polymers will adopt an open random coil configuration. Thus, the *D*_h of the polymers in acetone should be larger than those in water because the random coil polymers have larger spatial conformation than the more compact SCPNs. Indeed, the polymers recorded *D*_h values of 2.6-3.3 nm and 1.0-1.4 nm in acetone and water, respectively (Figure 1c, Table 1). The 58-64% reductions in size indicated the formation of SCPNs in water, irrespective of the types of cationic or hydrophobic groups. To visualize the morphology of SCPNs, AFM analysis was performed on P_{Dab-F} as an example. The topography of the SCPN, which was drop-casted onto a silicon wafer, revealed distinct particulate entities (Figure 2a,c). Inspection of the AFM height profile revealed the SCPNs were ca. 1.8 nm tall on average, almost double the *D*_h value measured by DLS (Figure 2b). The discrepancy may be explained by the fact that AFM measurement was performed in the dried state, hence the topology and size of the nanoparticles may be different compared to when they were in the wet state. Further, drying effects may have also contributed to some agglomeration of the nanoparticles, thereby resulting in larger size distribution. It is also worth noting that the enhanced widths of the nanoparticles were due to deconvolution effects and therefore cannot be used for estimating the diameter of the nanoparticles.³³⁻³⁶ Visualization of SCPNs is often challenging, as observed by others.³³⁻⁴⁰ Nonetheless, the combined DLS and AFM results sufficiently demonstrate the formation of SCPNs in this study. Meanwhile, zeta potential (*ζ*) analysis showed the SCPNs have similar *ζ* values (25-33 mV) regardless of the types of cationic and hydrophobic groups (Table 1).

Table 1. Polymer Characterization by NMR, GPC, DLS and Zeta Potential Analysis

| Entry | <i>M</i> _n ^{a,b} (g mol ⁻¹) | <i>M</i> _n ^{a,c} (g mol ⁻¹) | <i>D</i> ^{a,c} | <i>D</i> _h ^{d,e} (nm) | <i>D</i> _h ^{d,f} (nm) | <i>ζ</i> ^{d,f} (mV) |
|----------------------|---|---|-------------------------|---|---|------------------------------|
| P _{Dab-L} | 27900 | 11200 | 1.3 | 3.3 | 1.2 | 32 |
| P _{Dab-F} | 27800 | 10200 | 1.3 | 2.6 | 1.0 | 27 |
| P _{Dab-EH} | 27900 | 13100 | 1.2 | 3.0 | 1.1 | 25 |
| P _{Dab-Pyr} | 30100 | 10500 | 1.3 | 2.8 | 1.0 | 27 |

| | | | | | | |
|------------|-------|-------|-----|-----|-----|----|
| P_{K-L} | 28500 | 11300 | 1.3 | 3.2 | 1.3 | 33 |
| P_{K-F} | 30000 | 10700 | 1.3 | 3.2 | 1.0 | 30 |
| P_{K-EH} | 29300 | 12300 | 1.3 | 3.3 | 1.4 | 31 |

^aBased on Boc-protected polymers. ^bDetermined via ¹H NMR analysis. ^cDetermined via GPC analysis in tetrahydrofuran solvent. ^dBased on Boc-deprotected polymers. ^eAnalysis performed in acetone. ^fAnalysis performed in water.

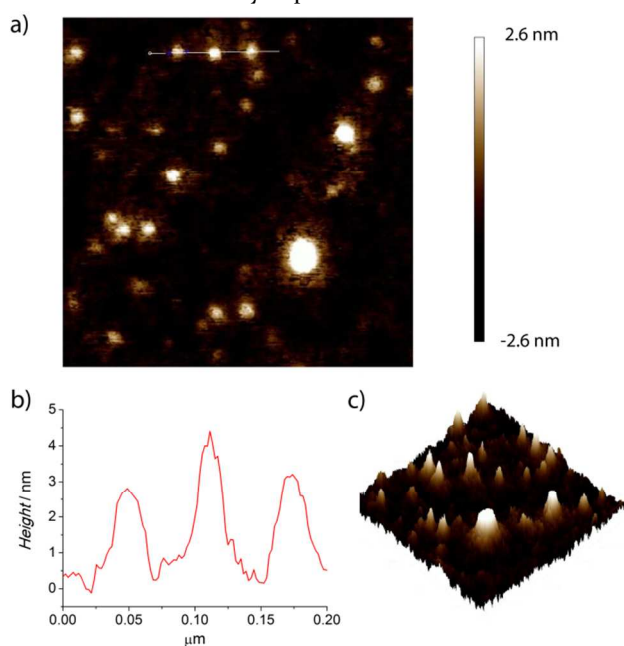


Figure 2. (a) AFM topography image (600 × 600 nm) of SCPN P_{Dab-F} on Si wafer. (b) The height-profile of the nanoparticles across the white line of the 2D AFM image in (a). (c) 3D height image (600 × 600 nm) of the nanoparticles in (a).

The in vitro antibacterial activity of the SCPNs against planktonic Gram-negative bacteria *Pseudomonas aeruginosa* and *Escherichia coli* was evaluated by determining their minimum inhibitory concentrations (MICs) in Mueller-Hinton broth (MHB), which is a nutrient rich bacterial growth media typically used in microbiology studies. The MIC is defined as the minimum drug concentration that prevents bacteria growth. It is worthwhile noting that we focused on Gram-negative pathogens (especially *P. aeruginosa*) as they are difficult to kill and infections caused by Gram-negative bacteria are considered more critical than those caused by Gram-positive bacteria nowadays due to the lack of new antibiotics that target the former.⁵⁰⁻⁵¹ Based on the MIC values in Table 2, we made several key observations.

Table 2. Antimicrobial Activity and Mammalian Cell Biocompatibility of Polymers and Antibiotics

| Entry | MIC ($\mu\text{g mL}^{-1}$ [μM]) ^a | | | | IC ₅₀ ($\mu\text{g mL}^{-1}$) | HC ₅₀ ($\mu\text{g mL}^{-1}$) | TI ^b | |
|------------------|---|-------------------|--------------------|-----------------------|--|--|-----------------------|-----------------------|
| | <i>P. aeruginosa</i> | <i>E. coli</i> | <i>V. cholerae</i> | <i>S. maltophilia</i> | H4IIE | RBC | IC ₅₀ /MIC | HC ₅₀ /MIC |
| P_{Dab-L} | 64-128 [2.3-4.6] | 128 [4.6] | n.d. | n.d. | 1200 | > 2000 | 9.4-18.8 | > 15.6 |
| P_{Dab-F} | 64-128 [2.3-4.6] | 32-64 [1.2-2.3] | > 128 [> 4.6] | > 128 [> 4.6] | 711 | > 2000 | 5.6-11.1 | > 15.6 |
| P_{Dab-EH} | 32-64 [1.1-2.3] | 32 [1.1] | 128 [4.6] | 128 [4.6] | 318 | > 2000 | 5.0-9.9 | > 31.3 |
| $P_{Dab-Pyr}$ | 64 [2.1] | 64 [2.1] | n.d. | n.d. | 1400 | > 2000 | 21.9 | > 31.3 |
| P_{K-L} | > 128 [> 4.5] | n.d. ^c | n.d. | n.d. | 207 | n.d. | n.d. | n.d. |
| P_{K-F} | > 128 [> 4.3] | n.d. | n.d. | n.d. | 237 | n.d. | n.d. | n.d. |
| P_{K-EH} | 32-64 [1.1-2.2] | 32-64 [1.1-2.2] | n.d. | n.d. | 146 | > 2000 | 2.3-4.6 | > 31.3 |
| P_{C1} | > 128 [> 9.1] | > 128 [> 9.1] | n.d. | n.d. | > 1024 | n.d. | n.d. | n.d. |
| P_{C2} | > 128 [> 5.1] | > 128 [> 5.1] | n.d. | n.d. | 47 | n.d. | n.d. | n.d. |
| Col ^d | 16 [9.1] | n.d. | > 128 [> 73] | 32 [18] | 53 | n.d. | 3.3 | n.d. |
| Gm ^d | 4 [8.4] | n.d. | 64 [134] | 64 [134] | n.d. | n.d. | n.d. | n.d. |

^aThe strains used were *P. aeruginosa* PAO1, *E. coli* K12, *V. cholerae* S10 and *S. maltophilia* 002. The values in square brackets are the MIC values expressed in μM concentration. ^bThe TI is defined as the ratio of IC₅₀ or HC₅₀ to MIC against *P. aeruginosa*. ^cn.d. indicates 'not determined.' ^dCol = colistin methanesulfonate and Gm = gentamicin.

Firstly, the antimicrobial activity against *P. aeruginosa* and *E. coli* generally improved (from 128 to 32 $\mu\text{g mL}^{-1}$) with increasing polymer hydrophobicity, i.e. from isoamyl (P_{Dab-L} , P_{K-L}) to phenylethyl (P_{Dab-F} , P_{K-F}) and to ethylhexyl (P_{Dab-EH} , P_{K-EH}). This was further suggested by a control polymer P_{C1} which lacks hydrophobic groups that did not show any antimicrobial activity (> 128 $\mu\text{g mL}^{-1}$). However, $P_{Dab-Pyr}$, which contains pyrene as the most hydrophobic

group in the series, was an exception to this trend as the SCPN only registered MIC value of 64 $\mu\text{g mL}^{-1}$, no better than SCPNs with the second most hydrophobic groups (i.e., P_{Dab-EH} , P_{K-EH}). In addition, SCPNs with longer alkyl spacer groups (4 vs 2 $-\text{CH}_2-$) between the amine and polymer backbone did not result in better antimicrobial performance. In fact, P_{K-L} and P_{K-F} have no antimicrobial activity (> 128 $\mu\text{g mL}^{-1}$) compared to P_{Dab-L} and P_{Dab-F}

which have MIC values of 64-128 $\mu\text{g mL}^{-1}$. Based on the MIC results, we postulated that the SCPNs exert their antimicrobial activity through cell membrane disruption where the extent of this mechanism was influenced by the overall amphiphilicity of the polymers. Apart from $\text{P}_{\text{Dab-Pyr}}$, we believed that the incorporation of more hydrophobic groups into the SCPNs resulted in greater membrane disruption events which therefore led to better antimicrobial activity. To confirm this, membrane potential measurements was performed to assess the ability of the SCPNs to perturb the cytoplasmic membrane (CM) of *P. aeruginosa*. For this experiment, a carbocyanine dye 3,3'-diethyloxycarbocyanine iodide ($\text{DiOC}_2(3)$) was employed. $\text{DiOC}_2(3)$ exhibits red fluorescence when it accumulates in bacteria cytosol with active CM potential but the intensity decreases and shifts to green fluorescence as the bacteria losses membrane potential (due to disruption events). This loss in membrane potential, measured as the ratio of red-to-green fluorescence, indicates the extent of CM disruption. Untreated cells (i.e., in the absence of antimicrobial agents) displayed red-to-green fluorescence ratio of ca. 2.9, which is expected of 'healthy' bacteria cells (Figure 3). For treated cells, the ratio dropped and plateau at different values (1.1 or ≤ 0.6) depending on the compounds tested. The drop in fluorescence ratio confirmed that the SCPNs are capable of disrupting the bacteria CM. It was also clear that the SCPN $\text{P}_{\text{Dab-Pyr}}$ was only half as efficient in disrupting the CM of *P. aeruginosa* compared to SCPNs $\text{P}_{\text{Dab-L}}$, $\text{P}_{\text{Dab-F}}$, $\text{P}_{\text{Dab-EH}}$ and $\text{P}_{\text{K-EH}}$. This suggests that pyrene is not a suitable group for CM insertion even though it is very hydrophobic and $\text{P}_{\text{Dab-Pyr}}$ most likely exerts its antimicrobial activity mainly through other mechanisms, which would explain why the polymer did not fit with the MIC trend in Table 2. Interestingly, the fluorescence ratio of $\text{P}_{\text{Dab-Pyr}}$ is similar to the aminoglycoside gentamicin which primarily acts by inhibiting protein synthesis in bacteria.⁵² Although $\text{P}_{\text{Dab-L}}$, $\text{P}_{\text{Dab-F}}$, $\text{P}_{\text{Dab-EH}}$ and $\text{P}_{\text{K-EH}}$ have similar fluorescence ratio values, we believed that the extent of CM disruption may have been proportional to the difference in hydrophobicity between isoamyl, phenylethyl and ethylhexyl groups. However, limitations to the assay sensitivity prevented us from accurately distinguishing the fluorescence ratio between $\text{P}_{\text{Dab-L}}$, $\text{P}_{\text{Dab-F}}$, $\text{P}_{\text{Dab-EH}}$ and $\text{P}_{\text{K-EH}}$. It is noteworthy that these SCPNs have similar fluorescence ratio to the 'last resort' antibiotic colistin methanesulfonate which is known to cause the disruption of bacteria CM.⁵³⁻⁵⁴

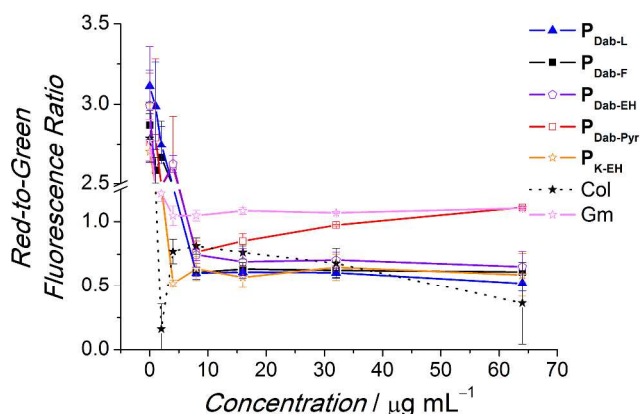


Figure 3. Cytoplasmic membrane potential measurements indicating the red-to-green fluorescence ratio of cells in the presence of different amounts of SCPNs and antibiotics colistin methanesulfonate (Col) and gentamicin (Gm).

Next, we noticed that polymer P_{C_2} , which is an OEG-less version of $\text{P}_{\text{Dab-F}}$, was inactive against *P. aeruginosa* and *E. coli*. This was because P_{C_2} formed polymer-protein complexes (PPCs) with proteins in MHB as evidenced by DLS analysis (Figure 4), which rendered the polymer ineffective towards bacteria. Recently, several studies on anti-cancer drug delivery systems have shown the formation of PPCs or protein corona on the surface of nanoparticles can severely reduce the potency of the materials as key functional groups, which are responsible for imparting specific biological activity, are masked.⁵⁵⁻⁵⁶ When SCPNs $\text{P}_{\text{Dab-F}}$ and $\text{P}_{\text{Dab-Pyr}}$ were mixed with MHB, peaks attributed to these PPCs (at ca. $D_h = 200$ nm) were undetectable in DLS. The same outcome was obtained for $\text{P}_{\text{Dab-F}}$ and $\text{P}_{\text{Dab-Pyr}}$ (i.e., no PPC formation) when Dulbecco's Modified Eagle Medium (DMEM) supplemented by 10% fetal bovine serum (FBS), which is a cell culture media typically used for mammalian cell culture studies, was used to ascertain the protein complexation behavior of the SCPNs in the presence of serum (Figure S8, SI). Additionally, the MIC values of $\text{P}_{\text{Dab-F}}$ and $\text{P}_{\text{Dab-Pyr}}$ samples that were pre-incubated in DMEM plus 10% FBS media were unaffected, indicating that the SCPNs can maintain their activity even in *in vivo* mimicking conditions. These results clearly show the incorporation of OEG (or potentially other low-fouling components) into the design of antimicrobial polymers is important in preventing the formation of PPCs and to preserve antimicrobial activity. This is an extremely crucial point to consider for potential clinical applications as the omnipresence of proteins in the body could significantly reduce the efficacy of an antimicrobial agent due to the formation of PPCs.

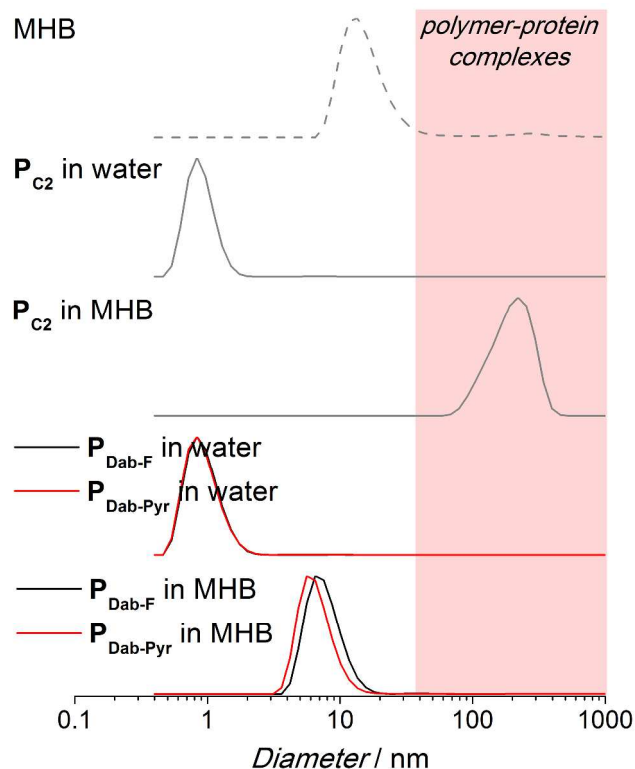


Figure 4. DLS volume distributions of P_{C2} (no OEG side chains) and SCPNs P_{Dab-F} and $P_{Dab-Pyr}$ (with OEG side chains) in water and MHB bacterial cell culture media.

Further inspection of the MICs in Table 2 revealed that the MICs of the most potent SCPNs P_{Dab-EH} and P_{K-EH} ($32\text{--}64\ \mu\text{g mL}^{-1}$) were higher than the MICs of the antibiotics colistin ($16\ \mu\text{g mL}^{-1}$) and gentamicin ($4\ \mu\text{g mL}^{-1}$) against *P. aeruginosa*. Although mass concentrations were conventionally used to determine antimicrobial activity, it is important to note that if the MICs in this study were reported in terms of molarity to account for the large difference in molecular weights between the SCPNs and commercial antibiotics, and for a more direct molecule-to-molecule comparison, P_{Dab-EH} and P_{K-EH} (as well as P_{Dab-L} , P_{Dab-F} , $P_{Dab-Pyr}$) actually possessed better antimicrobial activity than colistin and gentamicin. To further ascertain the antimicrobial potency of the polymers, SCPNs P_{Dab-F} and P_{Dab-EH} were tested against two highly pathogenic Gram-negative species, *Vibrio cholerae* and *Stenotrophomonas maltophilia*. While P_{Dab-F} was non active against both these species, P_{Dab-EH} registered MIC values of $128\ \mu\text{g mL}^{-1}$, which was almost as potent as gentamicin ($64\ \mu\text{g mL}^{-1}$) in terms of mass concentrations. Interestingly, despite having a MIC of $32\ \mu\text{g mL}^{-1}$ against *S. maltophilia*, colistin was ineffective against *V. cholerae*. The overall MIC assay thus confirms the ability of SCPNs in combating a variety of Gram-negative bacteria.

An antimicrobial resistance study was subsequently performed to determine if *P. aeruginosa* could acquire resistance to the SCPNs. For this, bacterial cells were subjected to serial passaging in the presence of sub-MIC levels of SCPNs P_{Dab-L} , P_{Dab-F} , P_{Dab-EH} and $P_{Dab-Pyr}$ over a period of 22 days (Figure 5). Colistin and gentamicin were

also included for comparison. *P. aeruginosa* eventually developed minor resistance towards SCPNs P_{Dab-L} , P_{Dab-F} and P_{Dab-EH} where $4 \times$ MICs were required to effectively combat the resistant strains. For $P_{Dab-Pyr}$, $8 \times$ MIC was required, and resistance development in bacteria was the most rapid among the SCPNs tested. This was most likely attributed to the poorer ability of $P_{Dab-Pyr}$ to cause membrane disruption compared to the other SCPNs since resistance development in bacteria is hindered by this mode of action. Closer inspection of Figure 5 revealed that the rate of resistance acquisition decreased in the order of $P_{Dab-Pyr}$, P_{Dab-L} , P_{Dab-F} and P_{Dab-EH} . This in fact supports the notion that ethylhexyl groups are better than phenylalanine and leucine mimics in perturbing the CM of bacteria, and hence bestowing P_{Dab-EH} with better antimicrobial activity than P_{Dab-F} and P_{Dab-L} . In comparison, colistin only produced transient resistant mutants and the MIC remained the same after 22 days of serial passaging. This result confirms that resistance to colistin is not easily acquired. Gentamicin on the other hand was the worst performing compound as resistance was fully developed within 5 days and the MIC increased to $64 \times$ the original value. While *P. aeruginosa* acquired resistance towards the SCPNs, the level of resistance is considered minimal and the SCPNs were clearly more effective in curbing the generation of resistant mutant strains compared to the commercially available antibiotic gentamicin.

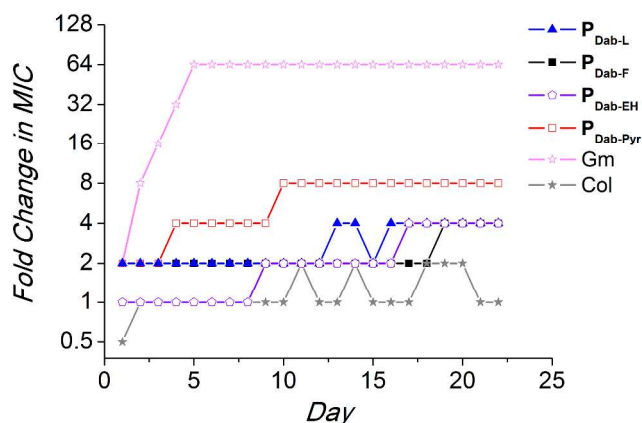


Figure 5. Antimicrobial resistance study that involves the serial passaging of *P. aeruginosa* in the presence of sub-MIC levels of various SCPNs and antibiotics. The y-axis represents the changes in MICs of the compounds as they were passaged over 22 days.

The biocompatibility of an antimicrobial agent is an important parameter that determines its applicability for real life usage. To test the mammalian cell biocompatibility of the SCPNs, rat H4IIE liver cells were used as a model cell line. MTS assay was conducted to determine the metabolic activity, which is an indicator of cell viability. Different concentrations of the polymers listed in Table 1 were dissolved in DMEM supplemented with 10% FBS and incubated with H4IIE cells for 24 h (Figure 6). At $128\ \mu\text{g mL}^{-1}$, SCPNs that displayed antimicrobial activity (i.e., P_{Dab-L} , P_{Dab-F} , P_{Dab-EH} , $P_{Dab-Pyr}$ and P_{K-EH}) have high mammalian cell viability ($\geq 80\%$). However, the viability de-

creased at higher polymer concentrations. The half maximal inhibitory concentration (IC_{50}), defined as the concentration of a substance where the biological response (e.g., cell viability) is reduced by half, was then determined (Table 2). The IC_{50} is typically used as a metric for determining the biocompatibility of a material. Similar to what was observed with the MIC values, the IC_{50} decreased with the increasing propensity of SCPNs to induce membrane disruption in bacteria cells. We believe that the SCPNs also perturb the membrane of mammalian cells albeit to a lesser extent. Interestingly, polymers that did not show antimicrobial activity (i.e., P_{K-L} , P_{K-F} and P_{C_2} (no OEG groups)) were cytotoxic toward H4IIE cells, whereas P_{C_1} (no hydrophobic groups) was benign to both bacteria and mammalian cells. Despite being a potent antimicrobial agent, colistin has very poor biocompatibility as evidenced by its low IC_{50} value ($53 \mu\text{g mL}^{-1}$). This is in contrast to P_{Dab-F} and P_{Dab-EH} which have IC_{50} values of 711 and $318 \mu\text{g mL}^{-1}$, respectively.

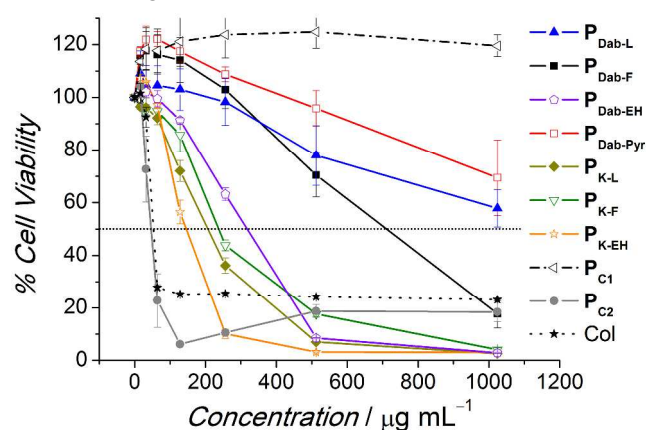


Figure 6. Percentage of living H4IIE cells after 24 h incubation with various compounds at different sample concentrations, as determined via MTT assay. The horizontal dashed line represents the cutoff point for determining the IC_{50} values of the compounds.

The hemolytic activity of the SCPNs was also determined using sheep red blood cells (RBCs). Similar to the definition of IC_{50} , the HC_{50} is defined as the sample concentration at which 50% of RBCs were lysed, and is commonly used as a standard for determining the hemolytic activity of biologically active compounds. All five SCPNs that were investigated (i.e., P_{Dab-L} , P_{Dab-F} , P_{Dab-EH} , $P_{Dab-Pyr}$, P_{K-EH}) were non-hemolytic even up to $2000 \mu\text{g mL}^{-1}$, indicating good cytocompatibility with RBCs. However, it must be noted that SCPNs P_{Dab-EH} and P_{K-EH} which consist of ethyl hexyl groups were the most hemolytic compared to the other polymers tested (30-40% vs $\leq 20\%$ of RBCs lysed at $2000 \mu\text{g mL}^{-1}$). The therapeutic index (TI) is another metric used to determine the biological performance of a drug. In this case, the TI was defined as the ratio of either IC_{50} to MIC (against *P. aeruginosa*) or HC_{50} to MIC. As seen in Table 2, the TI (IC_{50}/MIC) for colistin was only 3.3. Barring the lysine mimics (P_K series), the rest of the SCPNs have better TI (IC_{50}/MIC) values than colistin. In addition, the TI (HC_{50}/MIC) values for the

SCPNs were > 15.6 , thus highlighting the ability of the SCPNs to selectively target bacteria over RBCs.

Biofilms, as a network of bacteria cells protected by a matrix of extracellular substances, are more difficult to treat than their planktonic counterparts.⁵⁷ Thus, biofilm-related infections are often the main cause of chronic inflammations and recurrent infections.⁵⁸ Given that the SCPNs demonstrated good mammalian cell biocompatibility and antimicrobial activity on planktonic microbes, we investigated their ability to combat biofilms. The biofilms were grown in vitro in M9 minimal medium for 6 h prior to treatment with antimicrobial compounds. SCPNs P_{Dab-F} and P_{Dab-EH} were identified as the lead compounds taking into account their TI values and lowest probability for resistance development in bacteria, and hence were employed in biofilm studies. The bactericidal property of P_{Dab-F} and P_{Dab-EH} at $4 \times MIC$ in M9 (Table S1, S1) was assessed at different inoculation durations using colony-forming unit (CFU) analysis. It is noteworthy that the SCPNs have lower MIC values in M9 than in MHB media by 2-fold. Thus at this dosage, the SCPNs still possess favorable TI values. SCPNs P_{Dab-F} and P_{Dab-EH} displayed excellent bactericidal activity against both *P. aeruginosa* planktonic cells and biofilm, where a strong increase in the killing rate was observed when the bacterial cultures were treated for longer durations (Figure 7a,b).

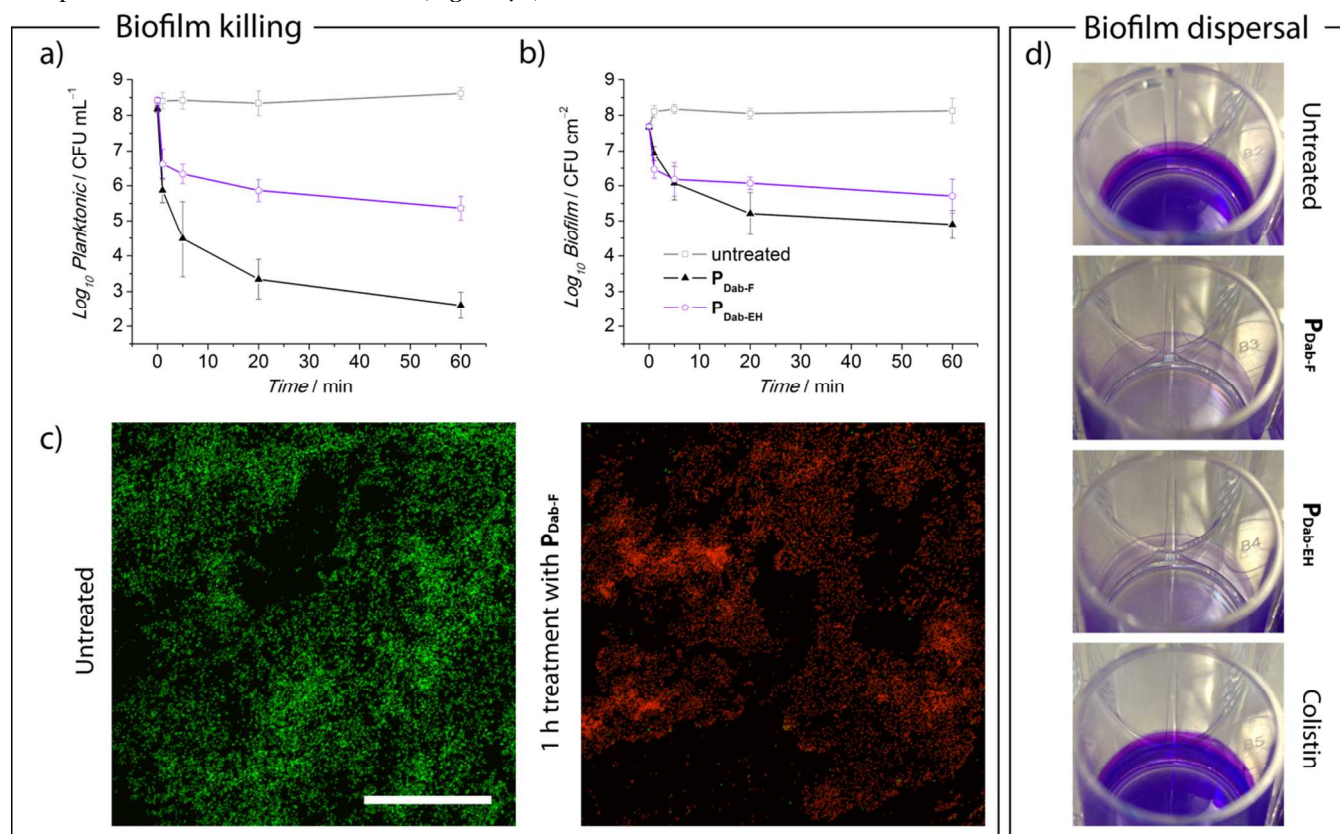
Firstly, the two SCPNs were assessed for their ability to kill the planktonic component of the biofilm-forming bacterial cultures. Treatment with P_{Dab-F} rapidly reduced the planktonic population from 2.1×10^8 CFU mL^{-1} (untreated cultures) to 6.7×10^5 CFU mL^{-1} within 1 min (Figure 7a). This translated to a 2.5-log_{10} reduction in CFU. Increasing the treatment duration to 20 min resulted in a greater decrease in the planktonic CFU to 2.2×10^3 CFU mL^{-1} , which equated to $> 5.0\text{-log}_{10}$ decrease in CFU compared to the untreated samples. After 60 min of treatment, the planktonic phase was further reduced to 4.9×10^2 CFU mL^{-1} . A total of 6.0-log_{10} reduction in planktonic CFU compared to untreated samples was observed after inoculating with P_{Dab-F} for 60 min. P_{Dab-EH} also displayed a very strong effect in killing planktonic cells though the efficiency was lower than P_{Dab-F} (Figure 7a). Bacterial cultures treated with P_{Dab-EH} for 60 min resulted in a 3.6-log_{10} reduction in CFU compared to the untreated cultures.

Next, we assessed the ability of P_{Dab-F} and P_{Dab-EH} in killing bacterial cells embedded in biofilms. Cultures treated with P_{Dab-F} and P_{Dab-EH} for 20 min have 1.3×10^5 biofilm CFU cm^{-2} and 1.2×10^6 biofilm CFU cm^{-2} , respectively. This translated to 3.0-log_{10} and 2.0-log_{10} reductions, respectively, compared to the untreated biofilms (1.3×10^8 CFU cm^{-2}). Prolonged treatment for 60 min resulted in a further decrease of biofilm CFU, i.e. to 3.3-log_{10} and 2.6-log_{10} reductions for P_{Dab-F} and P_{Dab-EH} , respectively (Figure 7b). In comparison, colistin ($4 \times MIC$) had negligible effect against biofilms. After 60 min of treatment with colistin, bacterial biofilms were reduced to 4×10^7 CFU cm^{-2} , which was $< 1.0\text{-log}_{10}$ reduction in biofilm CFU compared to the untreated controls (data not shown). In addition, confocal microscopy was used to ascertain the biofilm

1 killing activity of SCPNs. Biofilm cells were stained with LIVE/DEAD dyes, where live and dead bacteria appear green and red, respectively. Following a 60 min inoculation period, the biofilm surface treated with P_{Dab-F} revealed almost entirely dead cells (> 99%) compared to the untreated biofilms which showed only live cells (Figure 7c). Taken together, these results demonstrated the excellent bactericidal property of our SCPNs in combating *P. aeruginosa* planktonic cells and biofilm.

2 Interestingly, SCPNs P_{Dab-F} and P_{Dab-EH} were also capable of inducing the dispersal of *P. aeruginosa* biofilms. Preformed biofilms of the PAO1 strain that had been grown for 6 h were treated with P_{Dab-F} , P_{Dab-EH} and colistin for 20 and 60 min. The planktonic phase was discarded and the biofilm biomass was determined by crystal violet (CV) staining. The degree of staining on the well surfaces indicated that biofilms treated for 60 min with P_{Dab-F} and P_{Dab-EH} have significant reduction in biofilm biomass while those treated with colistin showed no difference compared to the untreated controls (Figure 7d). The CV-

3 stained biofilm biomass was quantified by measuring the optical density at 550 nm. Treatments with P_{Dab-F} and P_{Dab-EH} for 20 min led to $25.2 \pm 7.9\%$ and $24.5 \pm 6.3\%$ reduction in biomass respectively, compared to the untreated controls. When the biofilms were exposed to P_{Dab-F} and P_{Dab-EH} for 60 min, $72.5 \pm 5.4\%$ and $71.0 \pm 7.3\%$ of the biofilm biomass had been dispersed, respectively. In contrast, treatment with colistin induced an increase in the biofilm biomass by $12.6 \pm 7.0\%$ compared to the untreated controls. A higher concentration of colistin ($10 \times$ MIC) also failed to disperse the biofilm (data not shown). The additional ability of the SCPNs to disperse biofilms is particularly significant, as biofilm dispersal is perceived as a promising treatment strategy for combating biofilm-related infections. Once released from the biofilm, both dispersed cells and remaining biofilms are more susceptible to antimicrobial treatments and host immune defenses.⁴⁷ This is because antimicrobials are more effective against single-celled organisms and have better penetration into lower density, loosely-bound biofilms.



48 **Figure 7.** Bactericidal activity of SCPNs P_{Dab-F} and P_{Dab-EH} (at $4 \times$ MIC in M9 medium) on planktonic cells (a) and biofilm (b) was assessed by colony-forming unit (CFU) analysis. Data are representative of at least 3 independent experiments \pm s.d. (c) Confocal microscopy images of untreated and P_{Dab-F} treated biofilms stained with LIVE/DEAD (live cells appear green, dead cells appear red; scale bar = 100 μm). (d) Images of crystal violet-stained untreated biofilm and those treated with P_{Dab-F} , P_{Dab-EH} and colistin for 1 h.

54 CONCLUSIONS

55 In summary, well-defined linear random copolymers that consist of oligoethylene glycol (OEG), amine and hydrophobic groups were made, and underwent self-folding in water to form single-chain polymeric nanopar-

56 ticles (SCPNs). The nanoparticles are effective in combatting Gram-negative pathogens such as *Pseudomonas aeruginosa* and *Escherichia coli* at μM concentrations (e.g., 1.1 μM). We found that the combination of all three functionalities was integral to achieving optimum biological performance. Specifically, the hydrophobicity of the pol-

ymers influence membrane cell wall disruption which in turn affects antimicrobial activity and the rate of resistance acquisition in bacteria, whereas the presence of OEG side chains preserves the antimicrobial activity of the SCPNs in in vivo mimicking conditions by preventing undesirable protein complexation. Compared to colistin, which is regarded as the last line of defense against Gram-negative pathogens, the SCPNs generally possess better therapeutic index and hence better biocompatibility. Importantly, the main advantage of our SCPNs is their ability to kill both planktonic microbial cells and biofilm with $\geq 99.99\%$ efficiency within an hour. Most antimicrobial peptides and commercial antibiotics are impotent toward biofilms. Further, the SCPNs not only kill but also disperse biofilms (ca. 72% dispersal after 1 h treatment). The good antimicrobial properties and biocompatibility of the SCPNs, coupled with their synthetic ease, make them highly attractive for potential clinical applications. Work is currently underway in testing the SCPNs in animal model studies.

ASSOCIATED CONTENT

Supporting Information. Additional NMR, DLS, MIC and biofilm dispersal data are available in the Supporting Information. This material is available free of charge via the Internet at <http://pubs.acs.org>.

AUTHOR INFORMATION

Corresponding Authors

* E-mail: edgar.wong@unsw.edu.au (E.H.H.W.) and cboyer@unsw.edu.au (C.B.)

Author Contributions

The manuscript was written through contributions of all authors. All authors have given approval to the final version of the manuscript.

Notes

The authors declare no competing financial interest.

ACKNOWLEDGMENT

This work was supported by UNSW Australia and the Australian Research Council via the 2016 UNSW Vice-Chancellor's Research Fellowship (E.H.H.W.) and Future Fellowship (FT120100096, C.B.), respectively. We acknowledge the facilities and technical assistance provided by the Mark Wainwright Analytical Centre at UNSW Australia via the Nuclear Magnetic Resonance Facility (Dr. Donald Thomas and Dr. Adelle Amore), Electron Microscope Unit (Mr. Yin Yao), and Biomedical Imaging Facility. We also acknowledge some of the facilities provided by the Centre for Marine Bio-Innovation at UNSW.

REFERENCES

1. RSC News. Tackling antimicrobial resistance. <http://www.rsc.org/news-events/features/2015/may/tackling-antimicrobial-resistance/> (accessed September 2016).
2. Takahashi, H.; Palermo, E. F.; Yasuhara, K.; Caputo, G. A.; Kuroda, K. (2013) Molecular design, structures, and activity of antimicrobial peptide-mimetic polymers. *Macromol. Biosci.*, *13*, 1285-1299.

3. Payne, D. J.; Gwynn, M. N.; Holmes, D. J.; Pompliano, D. L. (2007) Drugs for bad bugs: confronting the challenges of antibacterial discovery. *Nat. Rev. Drug Discov.*, *6*, 29-40.
4. Wright, G. D. (2015) Solving the antibiotic crisis. *ACS Infect. Dis.*, *1*, 80-84.
5. Seil, J. T.; Webster, T. J. (2012) Antimicrobial applications of nanotechnology: methods and literature. *Int. J. Nanomedicine*, *7*, 2767-2781.
6. Lewis, K. (2012) Antibiotics: Recover the lost art of drug discovery. *Nature*, *485*, 439-440.
7. Ling, L. L.; Schneider, T.; Peoples, A. J.; Spoering, A. L.; Engels, I.; Conlon, B. P.; Mueller, A.; Schaberle, T. F.; Hughes, D. E.; Epstein, S.; Jones, M.; Lazarides, L.; Steadman, V. A.; Cohen, D. R.; Felix, C. R.; Fetterman, K. A.; Millett, W. P.; Nitti, A. G.; Zullo, A. M.; Chen, C.; Lewis, K. (2015) A new antibiotic kills pathogens without detectable resistance. *Nature*, *517*, 455-459.
8. Nichols, D.; Cahoon, N.; Trakhtenberg, E. M.; Pham, L.; Mehta, A.; Belanger, A.; Kanigan, T.; Lewis, K.; Epstein, S. S. (2010) Use of ichip for high-throughput in situ cultivation of "uncultivable" microbial species. *Appl. Environ. Microbiol.*, *76*, 2445-2450.
9. Boyer, C.; Corrigan, N. A.; Jung, K.; Nguyen, D.; Nguyen, T. K.; Adnan, N. N.; Oliver, S.; Shanmugam, S.; Yeow, J. (2016) Copper-mediated living radical polymerization (atom transfer radical polymerization and copper(o) mediated polymerization): from fundamentals to bioapplications. *Chem. Rev.*, *116*, 1803-1949.
10. Chen, M.; Zhong, M.; Johnson, J. A. (2016) Light-controlled radical polymerization: mechanisms, methods, and applications. *Chem. Rev.*, *116*, 10167-10211.
11. Braunecker, W. A.; Matyjaszewski, K. (2007) Controlled/living radical polymerization: features, developments, and perspectives. *Prog. Polym. Sci.*, *32*, 93-146.
12. Moad, G.; Rizzardo, E.; Thang, S. H. (2009) Living radical polymerization by the RAFT process - a second update. *Aust. J. Chem.*, *62*, 1402-1472.
13. Palermo, E. F.; Vemparala, S.; Kuroda, K. (2012) Cationic spacer arm design strategy for control of antimicrobial activity and conformation of amphiphilic methacrylate random copolymers. *Biomacromolecules*, *13*, 1632-1641.
14. Engler, A. C.; Shukla, A.; Puranam, S.; Buss, H. G.; Jreige, N.; Hammond, P. T. (2011) Effects of side group functionality and molecular weight on the activity of synthetic antimicrobial polypeptides. *Biomacromolecules*, *12*, 1666-1674.
15. Nederberg, F.; Zhang, Y.; Tan, J. P.; Xu, K.; Wang, H.; Yang, C.; Gao, S.; Guo, X. D.; Fukushima, K.; Li, L.; Hedrick, J. L.; Yang, Y. Y. (2011) Biodegradable nanostructures with selective lysis of microbial membranes. *Nat. Chem.*, *3*, 409-414.
16. Mizutani, M.; Palermo, E. F.; Thoma, L. M.; Satoh, K.; Kamigaito, M.; Kuroda, K. (2012) Design and synthesis of self-degradable antibacterial polymers by simultaneous chain- and step-growth radical copolymerization. *Biomacromolecules*, *13*, 1554-1563.
17. Oda, Y.; Kanaoka, S.; Sato, T.; Aoshima, S.; Kuroda, K. (2011) Block versus random amphiphilic copolymers as antibacterial agents. *Biomacromolecules*, *12*, 3581-3591.
18. Sgolastra, F.; Deronde, B. M.; Sarapas, J. M.; Som, A.; Tew, G. N. (2013) Designing mimics of membrane active proteins. *Acc. Chem. Res.*, *46*, 2977-2987.
19. Lienkamp, K.; Madkour, A. E.; Kumar, K. N.; Nusslein, K.; Tew, G. N. (2009) Antimicrobial polymers prepared by ring-opening metathesis polymerization: manipulating antimicrobial properties by organic counterion and charge density variation. *Chem. -Eur. J.*, *15*, 11715-11722.
20. Colak, S.; Nelson, C. F.; Nusslein, K.; Tew, G. N. (2009) Hydrophilic modifications of an amphiphilic polynorbornene and the effects on its hemolytic and antibacterial activity. *Biomacromolecules*, *10*, 353-359.

21. Lienkamp, K.; Kumar, K. N.; Som, A.; Nusslein, K.; Tew, G. N. (2009) "Doubly selective" antimicrobial polymers: how do they differentiate between bacteria? *Chem. -Eur. J.*, *15*, 11710-11714.
22. Zasloff, M. (2002) Antimicrobial peptides of multicellular organisms. *Nature*, *415*, 389-395.
23. Lam, S. J.; O'Brien-Simpson, N. M.; Pantarat, N.; Sulistio, A.; Wong, E. H. H.; Chen, Y. Y.; Lenzo, J. C.; Holden, J. A.; Blencowe, A.; Reynolds, E. C.; Qiao, G. G. (2016) Combating multidrug-resistant Gram-negative bacteria with structurally nanoengineered antimicrobial peptide polymers. *Nat. Microbiol.*, *1*, 16162.
24. Wong, E. H. H.; Khin, M. M.; Ravikumar, V.; Si, Z.; Rice, S. A.; Chan-Park, M. B. (2016) Modulating antimicrobial activity and mammalian cell biocompatibility with glucosamine-functionalized star Polymers. *Biomacromolecules*, *17*, 1170-1178.
25. Yang, C.; Krishnamurthy, S.; Liu, J.; Liu, S.; Lu, X.; Coady, D. J.; Cheng, W.; De Libero, G.; Singhal, A.; Hedrick, J. L.; Yang, Y. Y. (2016) Broad-spectrum antimicrobial star polycarbonates functionalized with mannose for targeting bacteria residing inside immune cells. *Adv. Healthc. Mater.*, *5*, 1272-1281.
26. Yuan, W.; Wei, J.; Lu, H.; Fan, L.; Du, J. (2012) Water-dispersible and biodegradable polymer micelles with good antibacterial efficacy. *Chem. Commun.*, *48*, 6857-6859.
27. Cobo, I.; Li, M.; Sumerlin, B. S.; Perrier, S. (2015) Smart hybrid materials by conjugation of responsive polymers to biomacromolecules. *Nat. Mater.*, *14*, 143-159.
28. Ren, J. M.; McKenzie, T. G.; Fu, Q.; Wong, E. H. H.; Xu, J.; An, Z.; Shanmugam, S.; Davis, T. P.; Boyer, C.; Qiao, G. G. (2016) Star polymers. *Chem. Rev.*, *116*, 6743-6836.
29. Lam, S. J.; Wong, E. H. H.; O'Brien-Simpson, N. M.; Pantarat, N.; Blencowe, A.; Reynolds, E. C.; Qiao, G. G. (2017) Bionano interaction study on antimicrobial star-shaped peptide polymer nanoparticles. *ACS Appl. Mater. Interfaces*, DOI: 10.1021/acsami.6b11402.
30. Ouchi, M.; Badi, N.; Lutz, J. F.; Sawamoto, M. (2011) Single-chain technology using discrete synthetic macromolecules. *Nat. Chem.*, *3*, 917-924.
31. Altintas, O.; Barner-Kowollik, C. (2016) Single-chain folding of synthetic polymers: a critical update. *Macromol. Rapid Commun.*, *37*, 29-46.
32. Gonzalez-Burgos, M.; Latorre-Sanchez, A.; Pomposo, J. A. (2015) Advances in single chain technology. *Chem. Soc. Rev.*, *44*, 6122-6142.
33. Altintas, O.; Willenbacher, J.; Wuest, K. N. R.; Oehlenschlaeger, K. K.; Krolla-Sidenstein, P.; Gliemann, H.; Barner-Kowollik, C. (2013) A mild and efficient approach to functional single-chain polymeric nanoparticles via photoinduced Diels-Alder ligation. *Macromolecules*, *46*, 8092-8101.
34. Dirlam, P. T.; Kim, H. J.; Arrington, K. J.; Chung, W. J.; Sahoo, R.; Hill, L. J.; Costanzo, P. J.; Theato, P.; Char, K.; Pyun, J. (2013) Single chain polymer nanoparticles via sequential ATRP and oxidative polymerization. *Polym. Chem.*, *4*, 3765-3773.
35. Whitaker, D. E.; Mahon, C. S.; Fulton, D. A. (2013) Thermoresponsive dynamic covalent single-chain polymer nanoparticles reversibly transform into a hydrogel. *Angew. Chem., Int. Ed.*, *52*, 956-959.
36. Wong, E. H. H.; Lam, S. J.; Nam, E.; Qiao, G. G. (2014) Biocompatible single-chain polymeric nanoparticles via organo-catalyzed ring-opening polymerization. *ACS Macro Lett.*, *3*, 524-528.
37. Wong, E. H. H.; Qiao, G. G. (2015) Factors influencing the formation of single-chain polymeric nanoparticles prepared via ring-opening polymerization. *Macromolecules*, *48*, 1371-1379.
38. Wedler-Jasinski, N.; Lueckerath, T.; Mutlu, H.; Goldmann, A. S.; Walther, A.; Stenzel, M. H.; Barner-Kowollik, C. (2017) Dynamic covalent single chain nanoparticles based on hetero Diels-Alder chemistry. *Chem. Commun.*, DOI: 10.1039/C6CC07427H.
39. Terashima, T.; Sugita, T.; Sawamoto, M. (2015) Single-chain crosslinked star polymers via intramolecular crosslinking of self-folding amphiphilic copolymers in water. *Polymer Journal*, *47*, 667-677.
40. Zhang, J.; Gody, G.; Hartlieb, M.; Catrouillet, S.; Moffat, J.; Perrier, S. (2016) Synthesis of sequence-controlled multiblock single chain nanoparticles by a stepwise folding-chain extension-folding process. *Macromolecules*, DOI: 10.1021/acs.macromol.6b01962.
41. Appel, E. A.; Dyson, J.; del Barrio, J.; Walsh, Z.; Scherman, O. A. (2012) Formation of single-chain polymer nanoparticles in water through host-guest interactions. *Angew. Chem., Int. Ed.*, *51*, 4185-4189.
42. Sanchez-Sanchez, A.; Arbe, A.; Colmenero, J.; Pomposo, J. A. (2014) Metallo-folded single-chain nanoparticles with catalytic selectivity. *ACS Macro Lett.*, *3*, 439-443.
43. Stals, P. J. M.; Gillissen, M. A. J.; Paffen, T. F. E.; de Greef, T. F. A.; Lindner, P.; Meijer, E. W.; Palmans, A. R. A.; Voets, I. K. (2014) Folding polymers with pendant hydrogen bonding motifs in water: the effect of polymer length and concentration on the shape and size of single-chain polymeric nanoparticles. *Macromolecules*, *47*, 2947-2954.
44. Terashima, T.; Sugita, T.; Fukae, K.; Sawamoto, M. (2014) Synthesis and single-chain folding of amphiphilic random copolymers in water. *Macromolecules*, *47*, 589-600.
45. Bai, Y.; Feng, X.; Xing, H.; Xu, Y.; Kim, B. K.; Baig, N.; Zhou, T.; Gewirth, A. A.; Lu, Y.; Oldfield, E.; Zimmerman, S. C. (2016) A highly efficient single-chain metal-organic nanoparticle catalyst for alkyne-azide "click" reactions in water and in cells. *J. Am. Chem. Soc.*, *138*, 11077-11080.
46. Nguyen, T.-K.; Selvanayagam, R.; Ho, K. K. K.; Chen, R.; Kutty, S. K.; Rice, S. A.; Kumar, N.; Barraud, N.; Duong, H. T. T.; Boyer, C. (2016) Co-delivery of nitric oxide and antibiotic using polymeric nanoparticles. *Chem. Sci.*, *7*, 1016-1027.
47. Nguyen, T. K.; Duong, H. T.; Selvanayagam, R.; Boyer, C.; Barraud, N. (2015) Iron oxide nanoparticle-mediated hyperthermia stimulates dispersal in bacterial biofilms and enhances antibiotic efficacy. *Sci. Rep.*, *5*, 18385.
48. Duong, H. T.; Jung, K.; Kutty, S. K.; Agustina, S.; Adnan, N. N.; Basuki, J. S.; Kumar, N.; Davis, T. P.; Barraud, N.; Boyer, C. (2014) Nanoparticle (star polymer) delivery of nitric oxide effectively negates *Pseudomonas aeruginosa* biofilm formation. *Biomacromolecules*, *15*, 2583-2589.
49. Willcock, H.; O'Reilly, R. K. (2010) End group removal and modification of RAFT polymers. *Polym. Chem.*, *1*, 149-157.
50. Taubes, G. (2008) The bacteria fight back. *Science*, *321*, 356-361.
51. Xu, Z. Q.; Flavin, M. T.; Flavin, J. (2014) Combating multidrug-resistant Gram-negative bacterial infections. *Expert Opin. Investig. Drugs*, *23*, 163-182.
52. Eustice, D. C.; Wilhelm, J. M. (1984) Mechanisms of action of aminoglycoside antibiotics in eucaryotic protein synthesis. *Antimicrob. Agents Chemother.*, *26*, 53-60.
53. Velkov, T.; Deris, Z. Z.; Huang, J. X.; Azad, M. A.; Butler, M.; Sivanesan, S.; Kaminskas, L. M.; Dong, Y. D.; Boyd, B.; Baker, M. A.; Cooper, M. A.; Nation, R. L.; Li, J. (2014) Surface changes and polymyxin interactions with a resistant strain of *Klebsiella pneumoniae*. *Innate Immun.*, *20*, 350-363.
54. Lee, H. J.; Bergen, P. J.; Bulitta, J. B.; Tsuji, B.; Forrest, A.; Nation, R. L.; Li, J. (2013) Synergistic activity of colistin and rifampin combination against multidrug-resistant *Acinetobacter baumannii* in an in vitro pharmacokinetic/pharmacodynamic model. *Antimicrob. Agents Chemother.*, *57*, 3738-3745.
55. Dai, Q.; Yan, Y.; Guo, J.; Björnalm, M.; Cui, J.; Sun, H.; Caruso, F. (2015) Targeting ability of affibody-functionalized

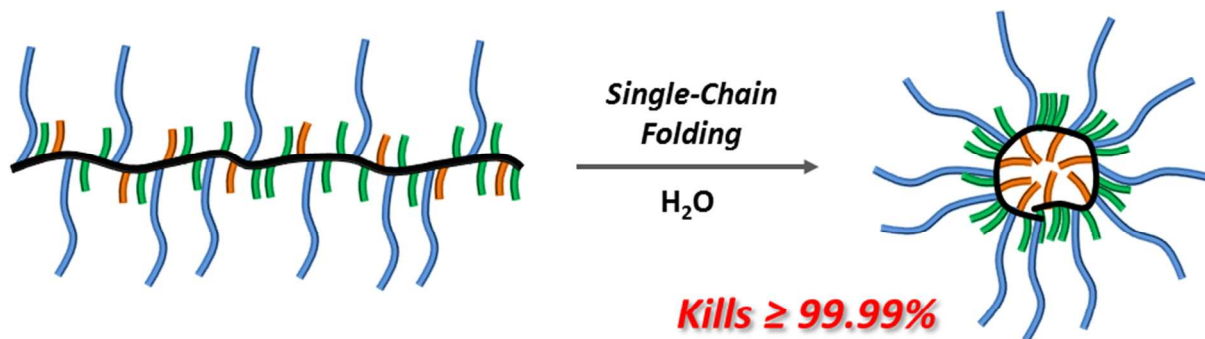
1 particles is enhanced by albumin but inhibited by serum
2 coronas. *ACS Macro Lett.*, 4, 1259-1263.

3 56. Salvati, A.; Pitek, A. S.; Monopoli, M. P.; Prapainop, K.;
4 Bombelli, F. B.; Hristov, D. R.; Kelly, P. M.; Aberg, C.; Mahon, E.;
5 Dawson, K. A. (2013) Transferrin-functionalized nanoparticles
6 lose their targeting capabilities when a biomolecule corona
7 adsorbs on the surface. *Nat. Nanotechnol.*, 8, 137-143.

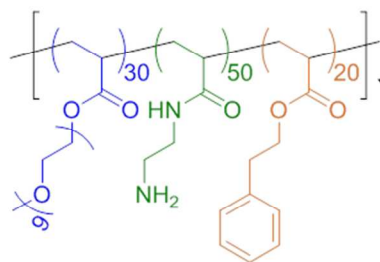
8 57. Hoiby, N.; Bjarnsholt, T.; Givskov, M.; Molin, S.; Ciofu,
9 O. (2010) Antibiotic resistance of bacterial biofilms. *Int. J.*
10 *Antimicrob. Agents*, 35, 322-332.

11 58. Costerton, J. W.; Stewart, P. S.; Greenberg, E. P. (1999)
12 Bacterial biofilms: a common cause of persistent infections.
13 *Science*, 284, 1318-1322.

For TOC Graphic



**Kills $\geq 99.99\%$
Bacteria in 1 h**



P_{Dab-F}

